

Design Procedure for the New 70-Meter Antenna Subreflector Positioner

R. D. Hughes

Ground Antenna and Facilities Engineering Section

Design procedures are developed for determining Cassegrain-type antenna subreflector positioner strength and displacements under wind and gravity loading conditions. The procedures are applied to the JPL 70-m antenna subreflector design, and the resulting design details are presented. The generalized analysis can be adapted to other antenna and subreflector-positioners. The results show that the new design meets the strength and displacements criteria under worst-case loading.

I. Introduction

Under the 64-meter to 70-meter Antenna Upgrade and Rehabilitation Project, the three existing 64-meter antennas of JPL at DSS-14 (Goldstone, California) DSS-43, (Tidbenbilla, Australia) and DSS-63 (Madrid, Spain) will undergo major modifications which will increase the antenna gain by 1.9 dB at X-band and extend the aperture diameter from 64 to 70 meters. Although the antenna will remain essentially Cassegrainian, the main reflector will be “shaped” to a slightly non-parabolic surface contour to provide a uniform RF radiation pattern. A uniform radiation pattern would increase the antenna gain and efficiency; and when added to other gain increases realized by extending the antenna diameter, resurfacing the main reflector by using high-precision surface panels, reduced quadripod blockage, and better subreflector controllers, will reach the 1.9 dB gain differential.

A new subreflector needed to be designed, therefore, which is larger in diameter and “shaped” also in such a manner that it will complement the main reflector shape to keep a constant beam path length and improve the RF performance. This sub-

reflector, hereafter referred to as the new 70-m antenna subreflector, will be heavier, subject to greater wind loading due to its increased surface area, and will be located in a different position relative to the quadripod apex when compared to the original 64-m antenna subreflector.

Thus, the need to re-design the subreflector positioner for the new 70-m antenna was inevitable. An analytical procedure was developed which characterizes the subreflector surface and its positioner as one assembly having load-displacement relationships described by a “structural flexibility matrix.” This flexibility matrix formulation then allows calculation of deflections and/or rotations of various components of the assembly for any given set of loading conditions. In this fashion, any component possessing excessive “compliance” will be noted, and the overall deflections and/or rotations of the subreflector relative to the apex will be determined.

Another part of the redesign process involved determining the new loads in each of the subreflector support shafts which connect the subreflector to the quadripod structure. The worst case loads were then used as criteria for the support shaft

design. This part of the design is presented in this report in terms of general analytical procedures which can be applied to other subreflector configurations in the antenna network.

In this report we present also the formulation of the subreflector loading conditions, the flexibility matrix, the general formulation of the procedure for the new 70-m subreflector positioner, a comparison of the strength versus loading of the subreflector support system, and the resulting key design details.

II. Design Procedure

For economic reasons, the new 70-m antenna subreflector positioner design was constrained such that the new positioner should resemble the existing 64-m antenna positioner in both configuration and mechanical details as closely as possible. Several alternative configurations were considered, primarily to provide a new, more flexible five degree-of-freedom subreflector motion (two lateral [x and y], one axial [z], and two tilting motions) as opposed to the three-degree-of-freedom motion with the existing 64-m antenna subreflector positioner (two lateral [x and y] and one axial [z]). However, the project cost and schedule requirements forced the new 70-m subreflector positioner design to have minimal impact on existing control system hardware and/or software. These have dictated further the installation of only a new three-degree-of-freedom positioner which can have provisions for future addition of a tilting mechanism.

Figure 1 shows the existing 64-m antenna subreflector-positioner configuration relative to the quadripod apex. The significant changes for the new 70-m antenna subreflector concern the new larger subreflector design and its new mounting provision. Details of the 70-m antenna subreflector design which will impact the positioner, e.g., new subreflector weight and size, were taken into account in this analysis. Figures 2 and 3 show the axial and lateral motion mechanisms which are analogous between the 64-m and 70-m designs. The major portion of the redesign effort has centered around determining adequacy of strength and magnitude deflections of all major components of the positioner under the worst cases of wind and/or gravity loading conditions.

A. Gravity and Wind Loads

The resultant loading matrix combining various antenna elevation angles and wind velocities and directions was calculated in two ways: first in terms of equivalent loads and moments at the subreflector and positioner centers-of-gravity, the results of which are used with the flexibility matrix to determine deflections and rotations of the subreflector relative to the apex; and second in terms of forces at the positioner support

shafts, z_1 , z_2 , z_3 , y_1 , y_2 , and x_1 shown in Figs. 2 and 3, the results of which are applied to the component strength analysis.

The sign conventions used for wind and gravity loading are shown in Fig. 4. For a given subreflector weight, W_s , and a given positioner suspended weight, W_p , the following relations express loads due to gravity:

$$\left. \begin{aligned} F_z &= -W_s \sin \alpha \\ F_y &= -W_s \cos \alpha \\ P_z &= -W_p \sin \alpha \\ P_y &= -W_p \cos \alpha \end{aligned} \right\} \quad (1)$$

where α = antenna elevation angle; F_y , F_z = loads at the subreflector center-of-gravity (c.g.) in the directions indicated by the subscripts corresponding to the coordinates system defined in Figs. 1-3; P_y , P_z = loads at the positioner c.g., analogous to F_y , F_z . For the 70-m antenna subreflector, $W_s = 10,400$ lb (46.26 kN) and $W_p = 6800$ lb (30.25 kN).

Wind loads were determined¹ and compiled from subsonic wind-tunnel experiments using a paraboloid dish in a uniform air stream. This wind loads computation approach is conservative, since for all antenna orientations, the subreflector is partially shielded (by the quadripod legs or the positioner) from direct wind, implying that actual wind loads are likely to be less than those calculated by wind-tunnel coefficients. Table 1 lists the force and moment coefficients and the resulting forces and moments for a 70 mph (112 km/h) wind, which is the survival wind velocity limit for any arbitrary antenna attitude.

For determining forces and moments from the wind coefficients data we use, for example:

$$\begin{aligned} F_D &= C_D q A \\ M_p &= C_m q A D \end{aligned} \quad (2)$$

where

F_D = drag force

q = dynamic pressure of wind (= $[1/2] \rho V^2$ where ρ is the air density and V is the wind velocity)

¹N. L. Fox, et al., Preliminary Report on Paraboloidal Reflector Antenna Wind Tunnel Tests (JPL Internal Memorandum), JPL - CP3 (Reorder No. 62-709), Jet Propulsion Laboratory, Pasadena, Calif., 1962.

A = subreflector aperture area

D = subreflector diameter

C_D = drag coefficient

M_p = pitch moment

C_m = moment coefficient

For the 70-m subreflector positioner, $A = 512.7 \text{ ft}^2$ (47.63 m²) and $D = 25.55 \text{ ft}$ (7.79 m).

Note that since the wind tunnel test data convention was that moments were considered about the subreflector vertex, and since the loading analysis requires moments about the torus c.g. (assumed to be at the intersection of the z-axis and the x-plane passing through the centerline of the torus), the equivalent moments were calculated from the data in Table 1 according to:

$$M_t = M_{SR} - LF \quad (3)$$

where

M_{SR} = a moment (pitch or yaw) about the subreflector vertex

M_t = equivalent moment at torus c.g.

L = axial distance between subreflector vertex and torus c.g.

F = lateral force at subreflector vertex

Combined wind and gravity equivalent loads are found significant, as shown in Table 2, for a wind velocity of 30 mph (48 km/h) which is the operational limit wind velocity.

For the second method in which loading conditions were expressed as forces in the positioner support shafts, the following gives the shaft forces for *gravity* loading:

$$\left. \begin{aligned} y_1 &= y_2 = \left(\frac{W_s + W_p}{2} \right) \cos \alpha \\ z_1 &= \frac{W_s L_3 \cos \alpha + (W_p + W_s) L_1 \cos \alpha}{L_1 + L_2} \\ z_2 &= z_3 = 1/2 \left[\frac{W_s L_3 \cos \alpha + (W_p + W_s) L_2 \sin \alpha}{L_1 + L_2} \right] \end{aligned} \right\} \quad (4)$$

where the variables are as defined in Fig. 4. For the 70-m positioner, $L_1 = 39.0 \text{ in.}$ (0.991 m), $L_2 = 56.0 \text{ in.}$ (1.422 m) and

$L_3 = 31.75 \text{ in.}$ (0.806 m). The following expressions give the shaft forces for *wind* loading:

$$\left. \begin{aligned} y_1 &= -F_L/2 + (L_2/L_5) F_y \\ y_2 &= -F_L/2 - (L_2/L_5) F_y \\ z_1 &= \frac{L_1}{L_1 + L_2} F_D + \frac{M_N}{L_1 + L_2} \\ z_2 &= 0.5 \left[\frac{L_2 F_D}{L_1 + L_2} + \frac{M_N}{L_4} - \frac{M_N}{L_1 + L_2} \right] \\ z_3 &= 0.5 \left[\frac{L_2 F_D}{L_1 + L_2} - \frac{M_N}{L_4} - \frac{M_N}{L_1 + L_2} \right] \end{aligned} \right\} \quad (5)$$

where

F_L = lift force

F_D = drag force

F_y = lateral force

M_p = pitch moment

M_N = yaw moment, according to Fig. 4

For the 70-m positioner, $L_4 = 53.0 \text{ in.}$ (1.35 m) and $L_5 = 110.0 \text{ in.}$ (2.79 m).

Shaft forces for combined gravity and wind loads are listed in Table 3 for a 70 mph (112 km/h) wind velocity at various antenna attitudes, and in Table 4 for a 100 mph (160 km/h) wind velocity at stow attitude (antenna at zenith, elevation angle = 90°). These conditions comprise the survivability limits in design. Worst-case loads from Tables 3 and 4 indicate a design load of 9953 lbs (443 kN) tension for the axial (z) positioner mechanism shafts, and 4482 lb (199 kN) tension and compression for the lateral (x-axis) positioner shaft. For design purposes, these loads were rounded off to 10,000 and 4500 lbs (445, 200 kN), respectively.

B. Strength of Mechanical Components

The mechanical components which connect the positioner-subreflector assembly to the quadripod structure comprise the positioner support system, and must withstand the loads due to gravity and wind. These loads are transmitted through the shaft assemblies for each of the three (x, y, and z) directions of positioner travel, according to the coordinate system shown in Figs. 1-3.

A shaft assembly consists of a rod, two universal joints, connecting hardware, and a ball-screw jack. The load-bearing

strength of each of these components was calculated by classical strength-of-materials methods, using simplifying assumptions where applicable. In some cases the manufacturer's rating is used for determining the strength of off-the-shelf components. Table 5 shows the load, strength, and factor of safety for support components. The only component having a marginal factor of safety (F. S.) is the y-axis screw jack, for which F. S. = 2.0. Since the strength of this component is based on the manufacturer's rating, which includes an additional factor of safety, the calculated factor of safety is considered adequate.

C. Design Details

All remaining components that are part of the positioner assembly were designed according to the previously discussed loading conditions. The following is a list of significant differences in subreflector design details between the old 64-m antenna and the new 70-m antenna positioners:

- (1) The lateral and axial support rod lengths will increase to conform to the new 70-m antenna geometry.
- (2) The y-axis lateral support shaft assembly will be upgraded to have mechanical strength equivalent to that of the z-axis assembly.
- (3) The y-axis drive motor assembly will be upgraded to provide 18 ft-lb (24.4 N-m) of torque at the output shaft (vs 12 ft-lb or 16.3 N-m) and output velocity of 0.90 rpm (vs. 0.45 rpm).
- (4) The gear reducer box, which is part of the positional readout assembly, will be modified to provide the proper synchro rotation rate.
- (5) The axial motion mechanism drive shaft which is parallel to the y-axis (Fig. 2, top view) will be segmented to allow for possible future modification of the axial drive to tilt the subreflector about the elevation axis.
- (6) The rotational drive mechanism and the index pin actuator will be changed from a pneumatically-driven to a mechanically-driven device.

III. Compliance Analysis

The motions of the subreflector relative to the main reflector which are induced by both gravity and wind loadings must be quantified for two reasons relating to improving the antenna performance:

- (1) Correctable motions will be compensated for by the subreflector positioner mechanism as controlled by the antenna servo controller. In the case of the new 70-m antenna positioner, z and y translations are

presently controlled to compensate for gravity-induced deflections, and the x-axis lateral motion mechanism is only used for manual alignment.

- (2) The remaining motions which are not correctable, such as the subreflector rotation, must not be excessive.

The results of a structural analysis using finite element computer models (such as JPL's IDEAS program) predict displacements of the quadripod apex relative to a best-fit paraboloid representing the main reflector. These displacements may be superimposed with the results of the positioner analysis to give overall relative motions required for the two reasons mentioned above. Thus, the required subreflector translations can be determined as a function of antenna elevation angle, and the resulting antenna performance may be estimated as described in Ref. 1.

A. Load-Displacement Relationship

Using the "force method" of structural analysis, the flexibility matrix of the positioner-subreflector assembly was computed to describe the load-displacement relationship for each component. The force method expresses the load-displacement relationship as:

$$\{\delta\} = [F] \{P\} \quad (6)$$

where $\{\delta\}$ is the displacement vector, consisting of translations and rotations of each major element of a structure (in this case, the positioner and the subreflector are the major elements); $[F]$ is the flexibility matrix, whose elements represent the displacements at a given point of the structure caused by the application of a *unit load* at any other point of the structure; $\{P\}$ is the load vector which consists of forces and moments at designated points on the structure.

Reference 2 describes the formulation of the flexibility matrix by summing the total strain energy contained in an externally loaded structure. The relationship described is written as:

$$[F] = [B]^T [f] [B] \quad (7)$$

where the matrix $[B]$ is the "static transformation matrix" given by:

$$\{p\} = [B] \{P\} \quad (8)$$

and where $[f]$ is a diagonal block matrix composed of elemental flexibility matrices; for example, for a system composed of three structural elements:

$$[f] = \begin{bmatrix} [f_a] & [0] & [0] \\ [0] & [f_b] & [0] \\ [0] & [0] & [f_c] \end{bmatrix} \quad (9)$$

For element a , for example, $\{\delta_a\} = [f_a] \{P_a\}$ where $\{\delta_a\}$ and $\{P_a\}$ are the displacement and load vectors pertaining particularly to element a . In Eq. (8), the vector $\{p\}$ is the vector of stress resultants which are caused by the application of loads $\{P\}$. The static transformation matrix is constructed by inspection such that Eq. (8) is satisfied.

B. New Positioner-Subreflector Displacements

The displacement and load vectors of Eq. (6) are given for the positioner subreflector assembly as:

$$\begin{aligned} \{\delta\}^T &= \{U_s \quad V_s \quad W_s \quad V_p \quad W_p \quad \theta_x \quad \theta_y\} \\ \{P\}^T &= \{F_x \quad F_y \quad F_z \quad P_y \quad P_z \quad M_x \quad M_y\} \end{aligned} \quad (10)$$

where U_s, V_s, W_s = displacements of the subreflector vertex in the x, y , and z directions; θ_x, θ_y are rotations of the subreflector about the x -axis and y -axis, respectively; F_x, F_y, F_z are loads at the subreflector c.g. caused by wind forces and subreflector weight; P_y, P_z = loads of the positioner c.g. due to positioner weight; M_x, M_y = moment about positioner c.g. caused by lateral loads at subreflector c.g.

The positioner-subreflector assembly was viewed as consisting of two structural elements: one element included the subreflector, the backup structure, and bearing adaptor ring; the other element consisted of the remaining positioner components up to the point of attachment to the apex. The stiffnesses of the major components in these elements were calculated either by classical strength-of-materials methods, or by computer model for the more complex items. Table 6 indicates the spring constants for translation and rotation of the subreflector, and Figs. 1-3 identify the components.

The spring constants were used to assemble the elements of the flexibility matrices, and the above procedure was applied to determine the overall flexibility matrix shown in Table 7. The calculated subreflector displacements relative to the apex are shown in Table 8 for both the gravity and 30 mph (48 km/h) wind loading conditions described in Table 2. To quantify the effect of wind loading, Table 9 is presented, giving displacements for gravity loading with no wind.

Note that worst cases of lateral translation, axial translation, and rotation were unchanged because the effect of wind

loading at 30 mph (48 km/h) was not sufficient to surpass the effect of worst-case gravity loading. This situation is due to the fact that worst-case wind loading occurs at orientations other than those at which worst-case gravity loading occur. A case with greater wind velocity will indicate worst-case displacements occurring at different antenna orientations.

For worst-case deflections. The method of calculating gain losses due to subreflector translation and rotation is as follows: The RMS equivalent gain loss for lateral (y) subreflector deflections is given by:

$$\text{RMS} = \frac{R_{\text{lat}} V_s}{m} \quad (11)$$

and for axial (z) subreflector deflections by:

$$\text{RMS} = \frac{R_{\text{ax}} W_s}{m} \quad (12)$$

where R_{lat} and R_{ax} are proportionality constants obtained from curves developed by radiation pattern analysis for a range of antenna configurations (Ref. 3), m is the magnification factor:

$$m = (c + a)/(c - a) \quad (13)$$

where

a = distance from the subreflector origin to the vertex (subreflector treated as a hyperboloid)

c = distance from the subreflector vertex to the virtual focus (hyperboloid focal length)

For the 70-m antenna, $a = 202.92$ in. (515.42 cm), $c = 272.37$ in. (691.82 cm), giving $m = 6.84$.

The gain loss in decibels is given by the relation developed by Ruze:

$$\text{dB} = -4.3429 \left(\frac{4 \pi \text{RMS}}{\lambda} \right)^2$$

For X-band operation, $\lambda = 1.396$ in. (3.546 cm). The pointing error is given by:

$$\theta_{px} = \frac{2 \theta_x (c - a) K}{f} \quad (14)$$

where θ_x = subreflector rotation, f = antenna focal length, and K = the beam deviation factor (Ref. 1). For the 70-m antenna, $f = 1072.0$ in. (2723 cm) and $K = 0.76$.

The equivalent gain losses corresponding to the root-mean-square (RMS) value of the main reflector surface distortion caused by subreflector translations, and the pointing error caused by subreflector rotation are indicated in Tables 8 and 9.

Displacements relative to the apex were used in calculating these performance parameters. Some subreflector displacements may actually be canceled by other antenna distortions. However, these RMS losses and pointing error values indicate relative subreflector-positioner structural integrity under various loading conditions.

IV. Summary

The method of analysis that was developed for determining adequacy of strength of the subreflector supports and displacements of the subreflector vertex under various antenna loading conditions were described in general. The method can be extended to other antenna designs, although some minor details may have to be modified to apply to other subreflector-positioner configurations.

The design of the new 70-m antenna subreflector-positioner has generated an additional product, the determination of subreflector motions relative to the quadripod apex, which will be used in the antenna alignment and pointing error reduction analysis.

References

1. Hughes, R. D. and Katow, M. S., Subreflector focussing techniques applied to new DSS-15 and DSS-45 34-m antennas, *TDA Progress Report 42-80*, Jet Propulsion Laboratory, Pasadena, Calif., October-December, 1984.
2. Levy, R. I., *Nuclear Weapons Effects on Shipboard Electronic Systems*, Department of the Navy, Washington D.C., May 24, 1962.
3. Katow, M. S., 34-meter antenna subreflector translations to maximize RF gain, *TDA Progress Report 42-62*, 112-120 January-February, 1981, Jet Propulsion Laboratory, Pasadena, CA.

Table 1. Net subreflector wind coefficients, forces, and moments at 70 mph (112 km/h) wind

Elev Angle, (deg)	Azimuth Angle, (deg)	Coefficients					Forces/Moments				
		C_D	C_L	C_Y	C_N	C_P	$F_{D'}$ klb (kN)	$F_{L'}$ lb (kN)	$F_{Y'}$ lb (kN)	M_N ft. lb (Nm)	$M_{P'}$ ft. lb (Nm)
0	0	1.5	0	0	0	0	9.4 (42)	0 (0)	0 (0)	0 (0)	0 (0)
0	60	1.58	0	0.29	-0.088	0	9.9 (44)	0 (0)	1.8 (8.1)	-14,133 (-19,164)	0 (0)
0	120	-0.20	0	0.39	0.138	0	-1.3 (-5.6)	0 (0)	2.5 (11)	22,163 (30,053)	0 (0)
30	0	1.46	-0.02	0	0	-0.04	9.2 (41)	-0.1 (-0.6)	0 (0)	0 (0)	-6,424 (-8,711)
45	0	1.48	0.11	0	0	-0.042	9.3 (41)	0.7 (3.1)	0 (0)	0 (0)	-6,745 (-9,146)
60	0	1.58	0.29	0	0	-0.088	9.9 (44)	1.8 (8.1)	0 (0)	0 (0)	-14,133 (-19,164)
90	0	-0.03	0.38	0	0	0.129	-0.2 (-0.8)	2.4 (11)	0 (0)	0 (0)	20,717 (28,092)

Notes: See Fig. 4 for definitions.

Antenna faces into wind for azimuth angle = 0.

Table 2. Equivalent subreflector loads: gravity + 30 mph (48 km/h) wind

Elev Angle, deg	Azimuth Angle, deg	F_x , lb (kN)	F_y , lb (kN)	F_z , lb (kN)	P_y , lb (kN)	P_z , lb (kN)
0	0	0 (0)	-10 (-46)	-1.7 (-7.7)	-6.8 (-30)	0 (0)
0	60	-2.0 (-8.9)	-10 (-46)	-1.8 (-8.1)	-6.8 (-30)	0 (0)
0	120	0.2 (0.7)	-10 (-46)	0.2 (1.0)	-6.8 (-30)	0 (0)
30	0	0 (0)	-8.6 (-38)	-6.9 (-31)	-5.9 (-26)	-3.4 (-15)
45	0	0 (0)	-6.5 (-29)	-9.1 (-40)	-4.8 (-21)	-4.8 (-21)
60	0	0 (0)	-3.2 (-14)	-10.8 (-48)	-3.4 (-15)	-5.9 (-26)
90	0	0 (0)	-0.1 (-0.5)	-10.4 (-46)	0 (0)	-6.8 (-30)

Note: F_x , F_y , F_z are forces acting at the subreflector c.g., including the effect of moments. P_y , P_z are forces acting at the positioner c.g.

Table 3. 70-m antenna subreflector positioner support loads: gravity + 70 mph (112 km/h) wind

Elev, deg	Azimuth, deg	Forces in Support Rods, klb (kN)					
		Z_1	Z_2	Z_3	Y_1	Y_2	X_1
0	0 ^a	7.4 (33)	1.0 (4.4)	1.0 (4.4)	8.6 (38)	8.6 (38)	0
0	60	7.6 (34)	-1.5 (-6.7)	3.9 (17)	9.5 (42)	7.7 (34)	1.8 (8.0)
0	120	3.0 (13)	-1.1 (-4.9)	-3.1 (-14)	9.9 (44)	7.4 (33)	2.5 (11)
30	0 ^a	9.6 (43)	4.1 (18)	4.1 (18)	7.5 (33)	7.5 (33)	0
45	0 ^a	10.0 (44)	5.8 (26)	5.8 (26)	5.7 (25)	5.7 (25)	0
60	0 ^a	8.9 (40)	8.0 (36)	8.0 (36)	2.6 (12)	2.6 (12)	0
90	0 ^a	8.0 (36)	6.5 (29)	6.5 (29)	-1.2 (-5.3)	-1.2 (-5.3)	0

^aAt AZ = 0, antenna points directly into wind.

Table 4. 70-m antenna subreflector positioner support loads: gravity + 100 mph (160 km/h) wind (stow condition)

Elev, deg	AZ, Deg	Forces in Support Rods, klb (kN)					
		Z_1	Z_2	Z_3	Y_1	Y_2	X_1
90	0	8.9 (39.7)	4.0 (17.6)	4.0 (17.6)	-2.4 (-10.9)	-2.4 (-10.9)	0
90	90	6.9 (30.7)	6.8 (30.0)	3.2 (14.0)	2.5 (11.1)	-2.5 (-11.1)	4.5 (19.9)
90	180	5.2 (23.2)	6.2 (27.5)	6.2 (27.5)	2.4 (10.9)	2.4 (10.9)	0
90	270	7.2 (32.1)	3.4 (15.1)	6.9 (30.7)	-2.5 (-11.1)	2.5 (11.1)	-4.5 (-19.9)

Table 5. 70-m antenna subreflector positioner support component strength

Component	Load, klb (kN)	Strength ^a klb (kN)	Factor of Safety
S/R Rotation Bearing	58.6 (260.5)	744.0 (3309.3) (R)	12.7
Axial Rods	10.0 (44.5)	68.4 (304.2) (Y)	6.8
Axial Universal Joint	10.0 (44.5)	54.0 (240.2) (R)	5.4
Axial U-Joint Pin	10.0 (44.5)	51.2 (227.8) (Y)	5.1
Lateral (y) Rod	10.0 (44.5)	45.0 (200.2) (Y)	4.5
Lateral (y) Universal Joint	10.0 (44.5)	39.0 (173.5) (R)	3.9
Lateral (y) U-Joint Pin	10.0 (44.5)	51.2 (227.8) (Y)	5.1
Lateral (x) Rod	4.5 (20.0)	45.0 (200.2) (Y)	10.0
Lateral (x) Universal Joint	4.5 (20.0)	39.0 (173.5) (R)	8.7
Lateral (x) U-Joint Pin	4.5 (20.0)	51.2 (227.8) (Y)	11.4
Axial Screw Jack	10.0 (44.5)	40.0 (177.9) (R)	4.0
Lateral (y) Screw Jack	10.0 (44.5)	20.0 (89.0) (R)	2.0
Lateral (x) Screw Jack	4.5 (20.0)	20.0 (89.0) (R)	4.4

^aBased on tensile yield stress (*y*) or rated capacity (*r*).

Table 6. 70-m antenna subreflector positioner spring constants

Component	Rotational (N/rad) $\times 10^8$			Translational (N/m) $\times 10^6$		
	K_{x-x}	K_{y-y}	K_{z-z}	K_x	K_y	K_z
Axial Adjustment Mech.	4.49	4.10	— —	— — —	— — —	267.9
Torus + Lateral Adjustment Mechanism	3.38	1.47	1.78	31.5	131.3	210.1
Torus-to-Bearing Adaptor	22.15	22.15	— —	— — —	— — —	6129.1
Rotation Bearing	21.0	21.0	— —	3502.4	3502.4	7004.7
Bearing-to-S/R Adaptor	58.70	58.70	— —	3467.3	3467.3	53060.8
Subreflector + Back-up Structure	9.10	9.10	— —	218.9	218.9	646.2

NOTE: Unlisted items are considered infinitely stiff. See Figs. 1-3 for definitions.

Table 7. 70-m antenna subreflector/positioner flexibility matrix load-displacement relationship (Eq. 6) given by: $\{\delta\} = [F] \{P\}$

(displacement vector = flexibility matrix • load vector)

$\left\{ \begin{array}{l} U_s, \text{ in. (m)} \\ V_s, \text{ in. (m)} \\ W_s, \text{ in. (m)} \\ V_p, \text{ in. (m)} \\ W_p, \text{ in. (m)} \\ \theta_x, \text{ rad} \\ \theta_y, \text{ rad} \end{array} \right\}$	$=$	$\left[\begin{array}{cccccccc} 9.33 \times 10^{-6} & 0 & 0 & 0 & 0 & 0 & 0 & 5.47 \times 10^{-8} \\ (5.33 \times 10^{-8}) & & & & & & & (1.23 \times 10^{-8}) \\ 0 & 3.96 \times 10^{-6} & 0 & 2.24 \times 10^{-5} & 0 & 3.67 \times 10^{-8} & 0 & \\ (2.26 \times 10^{-8}) & (1.28 \times 10^{-8}) & (1.28 \times 10^{-7}) & & (8.25 \times 10^{-9}) & & & \\ 0 & 0 & 1.81 \times 10^{-6} & 0 & 1.54 \times 10^{-6} & 0 & 0 & \\ (1.03 \times 10^{-8}) & (8.79 \times 10^{-9}) & & & & & & \\ 0 & 2.24 \times 10^{-6} & 0 & 1.38 \times 10^{-6} & 0 & 2.72 \times 10^{-8} & 0 & \\ (1.28 \times 10^{-8}) & (1.28 \times 10^{-8}) & (7.88 \times 10^{-9}) & & (6.12 \times 10^{-9}) & & & \\ 0 & 0 & 1.54 \times 10^{-6} & 0 & 1.54 \times 10^{-6} & 0 & 0 & \\ (8.79 \times 10^{-9}) & (8.79 \times 10^{-9}) & (8.79 \times 10^{-9}) & & & & & \\ 0 & 3.67 \times 10^{-8} & 0 & 2.72 \times 10^{-8} & 0 & 1.80 \times 10^{-10} & 0 & \\ (8.25 \times 10^{-9}) & (8.25 \times 10^{-9}) & (1.55 \times 10^{-10}) & & (1.59 \times 10^{-9}) & & & \\ 5.47 \times 10^{-8} & 0 & 0 & 0 & 0 & 0 & 1.8 \times 10^{-10} & \\ (1.23 \times 10^{-8}) & & & & & & (1.59 \times 10^{-9}) & \end{array} \right]$	$\left\{ \begin{array}{l} F_x, \text{ lb (N)} \\ F_x, \text{ lb (N)} \\ F_z, \text{ lb (N)} \\ P_y, \text{ lb (N)} \\ P_z, \text{ lb (N)} \\ M_x, \text{ in-lb (N-m)} \\ M_y, \text{ in-lb (N-m)} \end{array} \right\}$
--	-----	---	---

Table 8. Subreflector displacements relative to apex gravity + 30 mph (48 km/h) wind

Elev., deg	Azim, deg	$10^{-3} \frac{U_{s'}}{\text{in. (mm)}}$	$10^{-3} \frac{V_{s'}}{\text{in. (mm)}}$	$10^{-3} \frac{W_{s'}}{\text{in. (mm)}}$	$\theta_x, 10^{-3} \text{ rad}$	$\theta_y, 10^{-3} \text{ rad}$
0	0	0	-56 ⁽¹⁾ (-1.42)	-3 (-0.08)	-0.567	0
0	60	-19 (-0.48)	-56 (-1.42)	-3 (-0.08)	-0.567	-0.109 ⁽³⁾
0	120	2 (0.05)	-56 (-1.42)	-0.4 (-0.01)	-0.567	9.14×10^{-3}
30	0	0	-47 (-1.19)	-18 (-0.46)	-0.477	0
45	0	0	-37 (-0.94)	-24 (-0.61)	-0.369	0
60	0	0	-20 (-0.51)	-29 ⁽²⁾ (-0.74)	-0.210	0
90	0	0	-0.4 (-0.01)	-29 (-0.74)	-3.74×10^{-3}	0

NOTES:

- (1) RMS Equivalent Gain Loss = 1.5×10^{-4} in. (3.70×10^{-4} cm) or 7.48×10^{-6} db at X-band $\lambda = 3.546$ cm
(2) RMS Equivalent Gain Loss = 2.2×10^{-3} in. (5.59×10^{-4} cm) or 1.8×10^{-3} db at X-band $\lambda = 3.546$ cm
(3) Pointing Error = 1.07×10^{-5} rad (0.037 arc-minutes)

Table 9. Subreflector displacements relative to apex gravity only

Elev., deg	$10^{-3} \frac{U_{s'}}{\text{in. (mm)}}$	$10^{-3} \frac{V_{s'}}{\text{in. (mm)}}$	$10^{-3} \frac{W_{s'}}{\text{in. (mm)}}$	$\theta_x, 10^{-3} \text{ rad}$	$\theta_y, 10^{-3} \text{ rad}$
0	0	-56 ⁽¹⁾ (-1.42)	0	-0.567 ⁽³⁾	0
30	0	-49 (-1.24)	-15 (-0.38)	-0.491	0
45	0	-40 (-1.02)	-21 (-0.53)	-0.401	0
60	0	-28 (-0.71)	-25 (-0.64)	-0.283	0
90	0	0	-29 ⁽²⁾ (-0.74)	0	0

NOTES:

- (1) RMS Equivalent Gain Loss = 1.5×10^{-4} in. (3.70×10^{-4} cm) or 7.48×10^{-6} db at X-band $\lambda = 3.546$ cm
(2) RMS Equivalent Gain Loss = 2.2×10^{-3} in. (5.59×10^{-4} cm) or 1.8×10^{-3} db at X-band $\lambda = 3.546$ cm
(3) Pointing Error = 5.56×10^{-5} rad (0.19 arc-minutes)

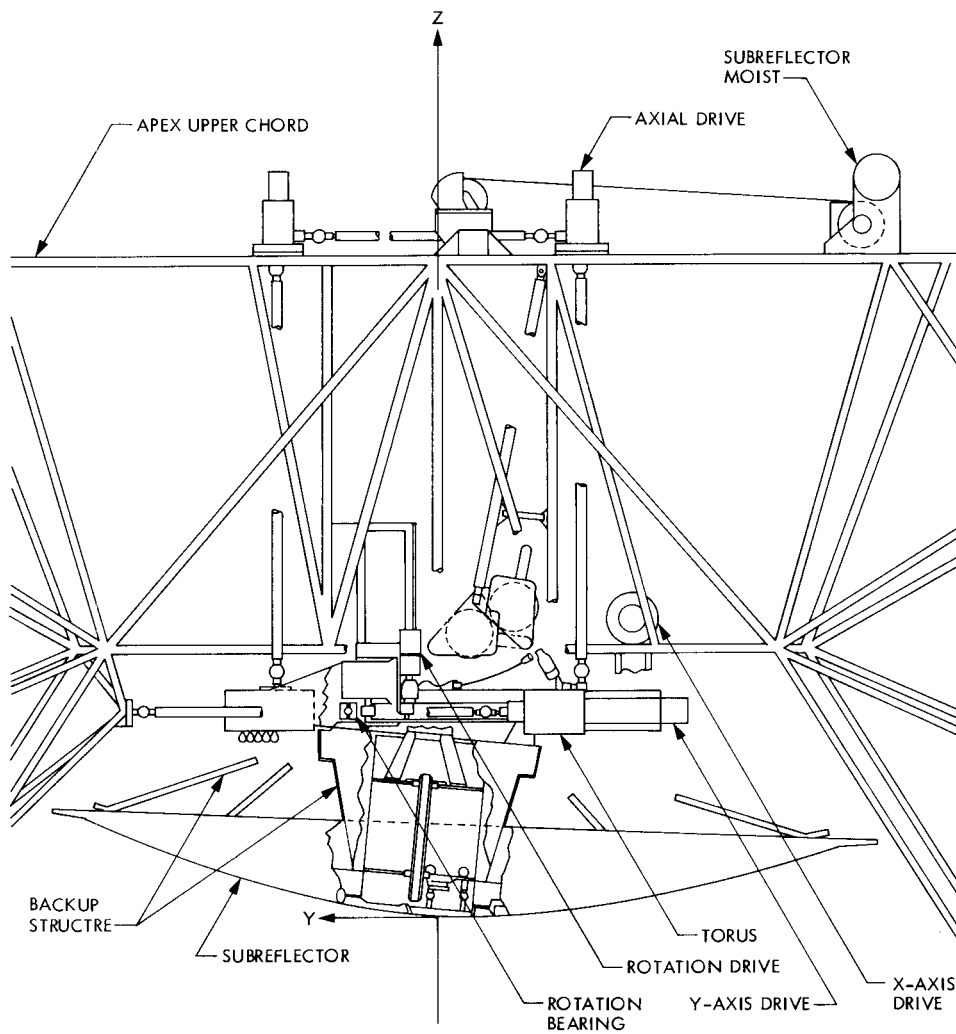


Fig. 1. Subreflector positioner mechanism

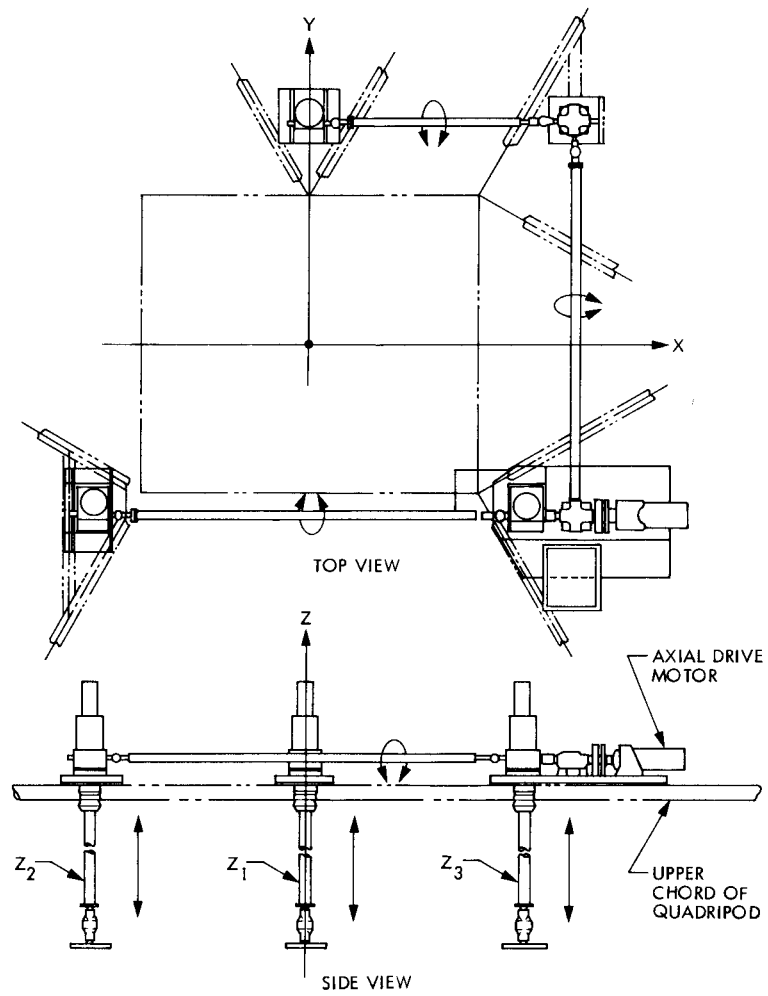


Fig. 2. Subreflector positioner axial motion mechanism

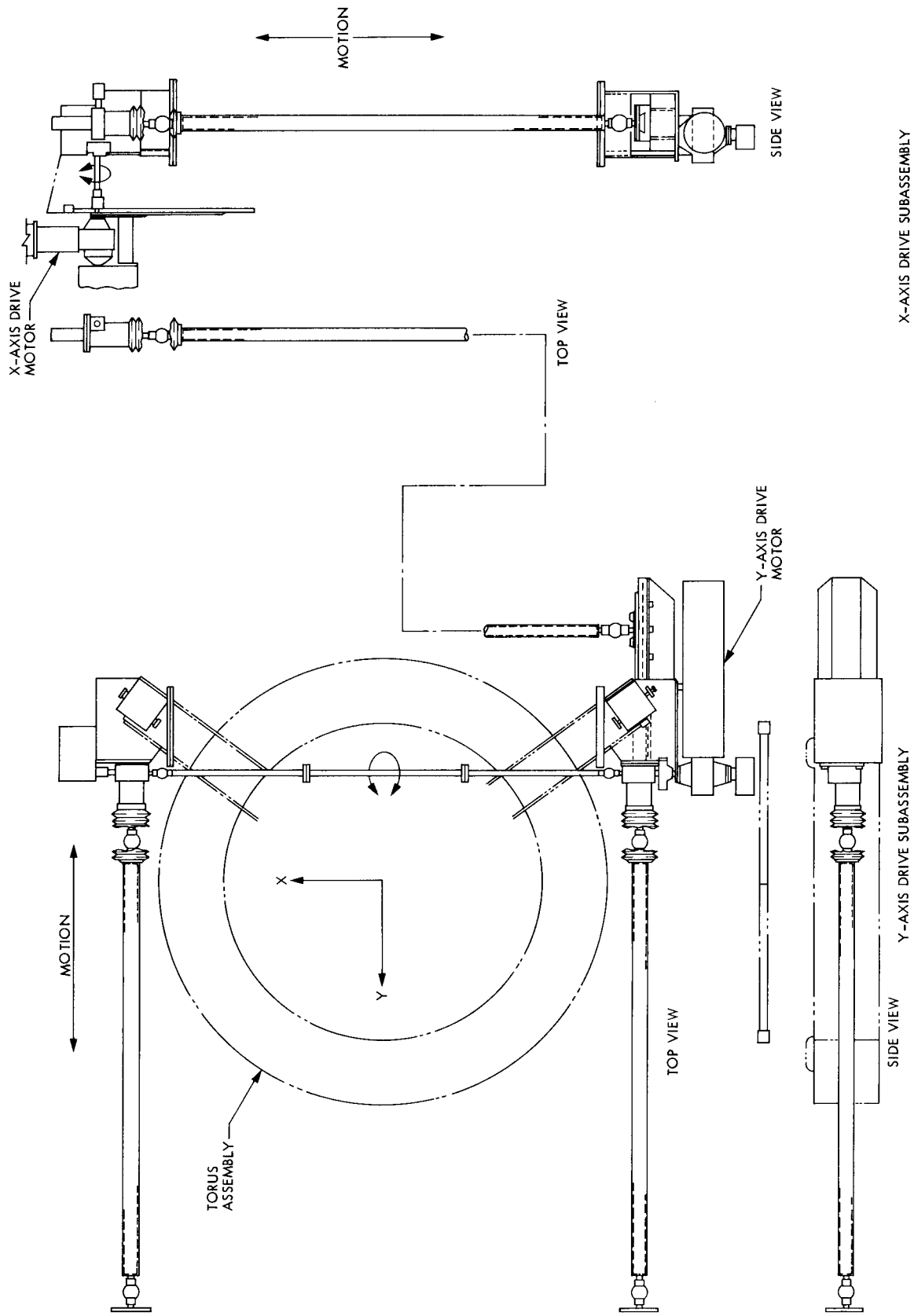
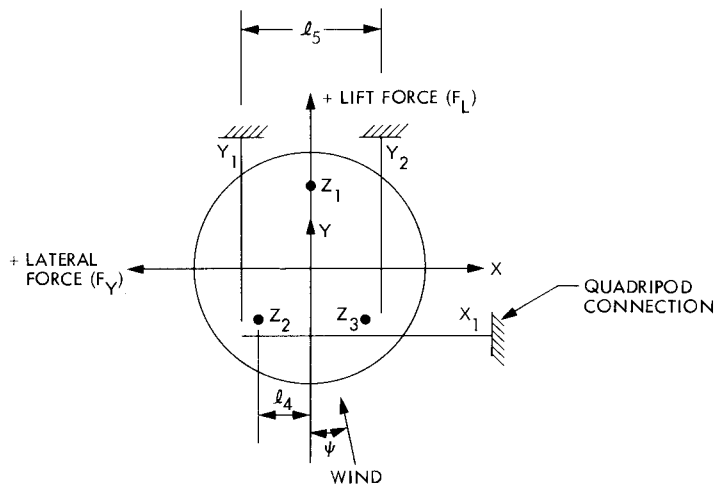
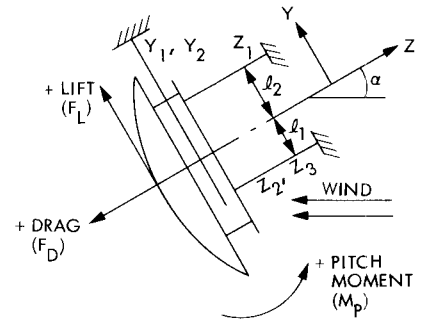


Fig. 3. Subreflector positioner lateral motion mechanism

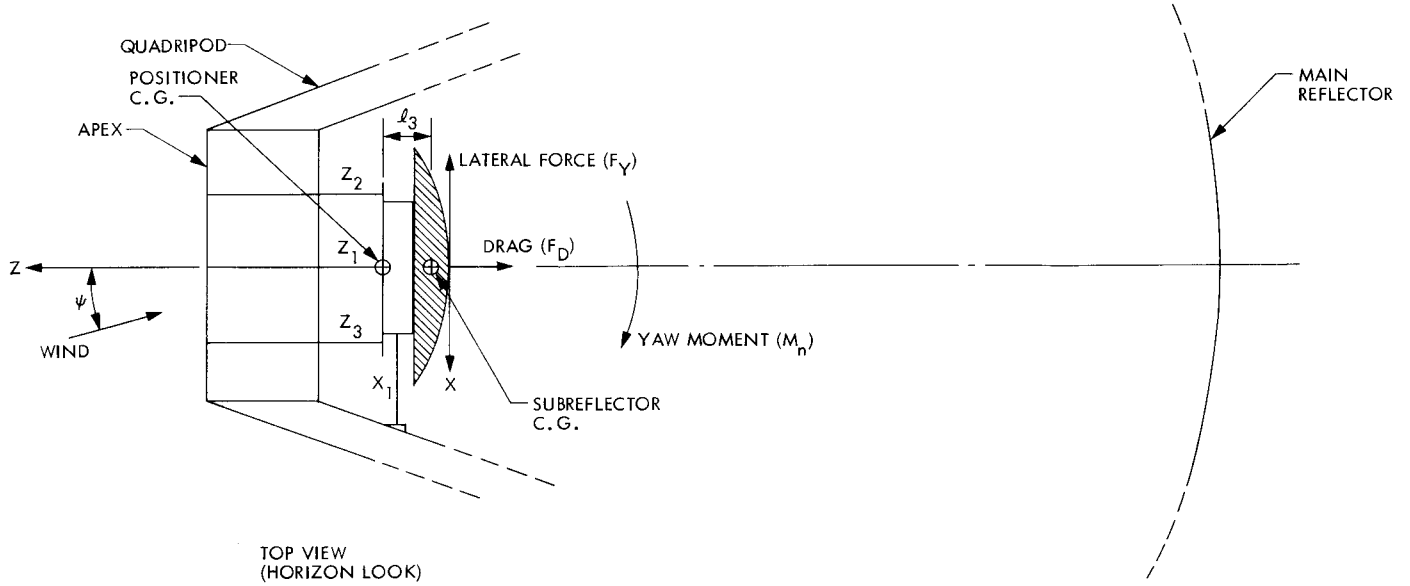


AXIAL VIEW, LOOKING FROM APEX
(ψ SHOWN FOR ZENITH LOOK)

NOTE : ψ = AZIMUTH ANGLE
 α = ELEVATION ANGLE



SIDE VIEW



TOP VIEW
(HORIZON LOOK)

Fig. 4. Wind and gravity force conventions